Imaging Intrinsic Diffusion of Bridge-Bonded Oxygen Vacancies on TiO_2(110)

Zhenrong Zhang,[1] Qingfeng Ge,[2] Shao-Chun Li,[3] Bruce D. Kay,[1] J. M. White,[1,3,*] and Zdenek Dohnálek[1,†]

[1]*Pacific Northwest National Laboratory, Fundamental Sciences Directorate, Chemical Sciences Division, Institute for Interfacial Catalysis, Richland, Washington 99352, USA*

[2]*Department of Chemistry and Biochemistry, Southern Illinois University, Carbondale, Illinois 62901, USA*

[3] *Department of Chemistry and Biochemistry, Center for Materials Chemistry, University of Texas at Austin, Austin, Texas 78712, USA*

(Received 3 April 2007; published 21 September 2007)

We report the first measurements and calculations of the *intrinsic* mobility of bridge-bonded oxygen (BBO) vacancies on a rutile TiO_2(110). The sequences of isothermal (340–420 K) scanning tunneling microscope images show that BBO vacancies migrate along BBO rows. The hopping rate increases exponentially with increasing temperature with an experimental activation energy of 1.15 eV. Density functional theory calculations are in very good agreement giving an energy barrier for hopping of 1.03 eV. Both theory and experiment indicate repulsive interactions between vacancies on a given BBO row.

DOI: 10.1103/PhysRevLett.99.126105 PACS numbers: 68.47.Gh, 68.37.Ef, 73.43.Cd, 82.65.+r

In the past two decades, titanium dioxide has emerged as an extremely promising material with numerous applications in such diverse and technologically important areas as heterogeneous catalysis, photocatalytic H_2O splitting, transparent coating for self-cleaning surfaces, and solar cells [1–4]. This widespread applicability has led to extensive fundamental and applied research aimed at understanding the underlying physical and chemical processes on pristine and doped forms of TiO_2. Despite extensive effort, numerous important questions about what properties control the TiO_2 activity remain unresolved. At a fundamental level, even the adsorption of simple molecules, for example, water, on the prototypical, rutile TiO_2(110) surface is still being actively investigated.

It is well established that the bridge-bonded oxygen (BBO) vacancy (BBO_V) sites which appear as defects in the BBO rows can play an important role in the catalytic activity of rutile TiO_2(110). These sites can be created during Mars–van Krevelen reactions that involve lattice oxygen as one of the reactants. Formally, creation of an oxygen vacancy by reduction leads to formation and exposure of two underlying Ti^{3+} ions. The spatial distribution of this extra charge has been calculated using density functional theory (DFT) but is still controversial [5–8].

Despite the fact that TiO_2(110) has been extensively studied with scanning tunneling microscopy (STM) [9–12] surprisingly little is known about the spatial distribution and/or mobility of the BBO_V sites. As shown recently [10], prior accounts of BBO_V diffusion [13,14] were in fact observations of the diffusion of hydrogen assisted by molecular water due to surface contamination from residual water in the UHV environment. This severe contamination problem is primarily caused by the near unit sticking probability of water on TiO_2(110) even at room temperature affecting TiO_2(110) studies in all but the cleanest UHV systems.

Here we take extreme care to prepare TiO_2(110) with negligible contamination by background water and employ isothermal (350–423 K) STM to obtain the first atomically resolved images revealing the dynamics of intrinsic oxygen vacancy motion. We demonstrate that the BBO_V's diffuse exclusively along the BBO rows with a hopping rate that increases exponentially with temperature. Arrhenius analysis yields a diffusion barrier of 1.15 eV in very good agreement with 1.03 eV obtained from DFT calculations.

Experiments were performed in an UHV chamber (base pressure $<8 \times 10^{-11}$ Torr) equipped with Omicron variable temperature STM, Auger electron spectroscopy (PHI), and quadrupole mass spectrometry (UTI). The TiO_2(110) ($10 \times 3 \times 2$ mm^3, Princeton Scientific) was mounted on a modified Omicron double plate sample holder and heated radiatively with a tungsten filament heater located behind the sample. Prior to use, commercial STM tips (tungsten, Custom Probe Unlimited) were cleaned via Ne^+ sputtering and UHV annealing. Well-ordered TiO_2(110) surfaces were prepared using repeated cycles of Ne^+ sputtering and UHV annealing at 900–950 K. To eliminate the influence of background H_2O (beyond maintaining a very low background pressure, 8×10^{-11} Torr), we placed a liquid nitrogen cooled surface near the substrate to cryogenically pump water. In addition, once the tunneling area A_0 was imaged, it was scanned with high sample bias (~3 V) to remove hydrogen from hydroxyl groups. All STM images (empty states) were collected using constant current (~0.1 nA) tunneling mode with a positive sample bias voltage (~1.0 V).

Periodic DFT calculations reported herein were performed using the VASP code [15]. We use projector augmented wave potentials [16] with the 3*d* and 4*s* valence states of Ti being expanded in a plane-wave basis set with a cutoff energy of 400 eV and PW91 form [17] of exchange-correlation functional. Theoretical derived lattice constants of rutile TiO_2 were used in the construction of slabs to model the surface oxygen vacancies. The reported barriers were calculated with one-sided slabs consisting of three O-Ti-O layers. We note that the calculated vacancy formation energy has been shown to depend on the slab thickness and unit cell size [18]. Our test calculations

with four O-Ti-O layers showed that the calculated barrier is converged within 30 meV. Spin polarization was necessary as the resulting states involving oxygen vacancies are in triplet states. Relaxing two trilayers in a 4-trilayer slab led to a singlet closed-shell state. Diffusional transition states were determined by a combined nudged elastic band method [19] and quasi-Newton optimization. Normal mode harmonic vibrational analysis was performed for the transition states and for selected initial geometries, and the calculated frequencies were used to estimate the diffusion prefactor [20].

The thermally driven intrinsic motion of BBO_V's along the BBO rows is revealed in Fig. 1. Figures 1(a) and 1(b) show two subsequent atomically resolved STM images from an extended sequence (see STM movie [21]) obtained on the same area of an adsorbate free $TiO_2(110)$ surface at 400 K. The corresponding ball models of the surface structure of selected areas marked by blue squares are overlaid on top of the images. The surface is composed of rows of topographically low lying Ti^{4+} ions (red) and rows of topographically high lying BBO ions (light blue) running along the [001] direction. In the empty state STM images, the low lying Ti^{4+} ions are imaged as protrusions while the rows of BBO ions are imaged as depressions due to the inverse electronic contrast of these two ions [9]. Additionally, the locations of five BBO_V's that appear on the image as bright protrusions are highlighted with arrows. The position of two BBO_V's (yellow arrows) changed from Fig. 1(a) to Fig. 1(b) as they moved along the [001] direction. The different position of the BBO_V is the result of movement of an adjacent BBO ion in the opposite direction.

The spatial distribution of all BBO_V's that move can be easily visualized by the subtraction of Fig. 1(b) from Fig. 1(a). In the difference image [Fig. 1(c)] the bright yellow protrusions indicate the original BBO_V positions [Fig. 1(a)] and the blue depressions indicate the new BBO_V positions [Fig. 1(b)] after they have moved. This difference image illustrates that the BBO_V's diffuse exclusively along the [001] direction and that all observed displacements between two consecutive images (2 min) range from 1 to 2 atom lattice spacings. Analysis of many images (~100) reveals that at 400 K about 50% of the BBO_V's change their position from image to image. Cross row hopping is never observed in the temperature range (350–423 K) explored here.

As the hopping rate h increases it becomes increasingly likely that a growing number of hops is undetected with our slow sampling rate (0.5–1 frame/min). For example, a zero net BBO_V displacement would result from two sequential hops in opposite directions. To account for this we use a mathematical analysis for a 1-dimensional (1D) random walk put forward by Wrigley and co-workers [22]. Here the probability $P_x(ht)$ of finding the diffusing entity displaced from its initial position by a displacement x at time t, is given by the following expression:

$$P_x(ht) = \exp(-2ht) I_x(2ht), \quad (1)$$

where I_n are modified Bessel functions of the first kind. The mean square displacement of the distribution $\langle \Delta x^2 \rangle$ is given as follows [23]:

$$\langle \Delta x^2 \rangle = 2ht. \quad (2)$$

We have determined the hopping rates as well as the overall distributions of BBO_V displacements using Eqs. (1) and (2) at seven different temperatures between 350 and 423 K. An example of the experimentally measured distributions determined at 400 K as well as the best fits obtained using Eqs. (1) and (2) are shown in Fig. 2. The good quality of the fit gives us confidence that the motion of the BBO_V's can be described by a simple 1D random walk.

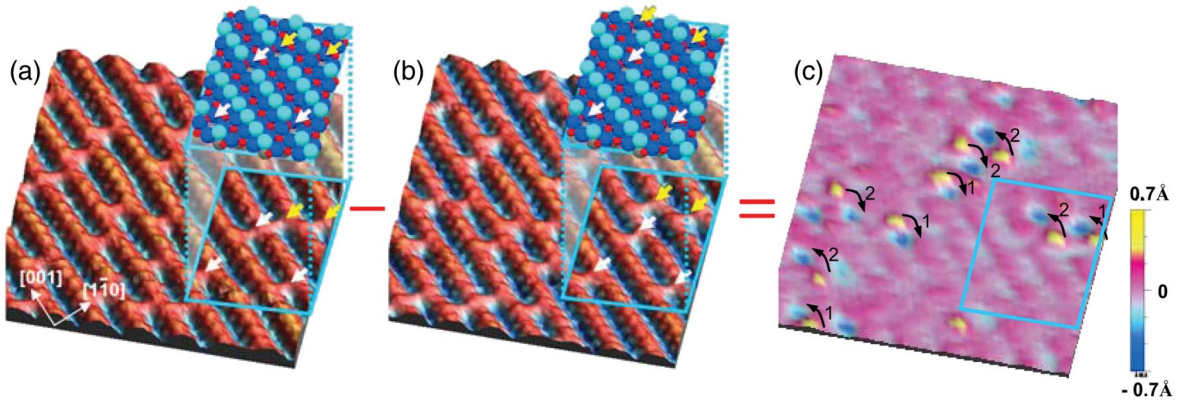

FIG. 1 (color). (a),(b) Two subsequent ($t = 2$ min) atomically resolved empty state STM images from an STM movie [21] obtained on the same area (64×69 Å^2) of clean $TiO_2(110)$ at 400 K. The distance between adjacent Ti^{4+} ions on the protruding row is 3.0 Å and distance between the Ti^{4+} rows is 6.5 Å. Superimposed are ball models of the $TiO_2(110)$ surface depicting regions of the STM images highlighted with blue squares. The rows of surface oxygen (bridge-bonded oxygen, BBO) ions are light blue, lattice oxygen ions dark blue, surface titanium (4+) ions red, and BBO vacancies (BBO_V's) marked with arrows. (c) Difference image, in which (b) is subtracted from (a); the blue depressions indicate the new BBO_V positions in (b) and the yellow protrusions indicate the original BBO_V positions in (a).

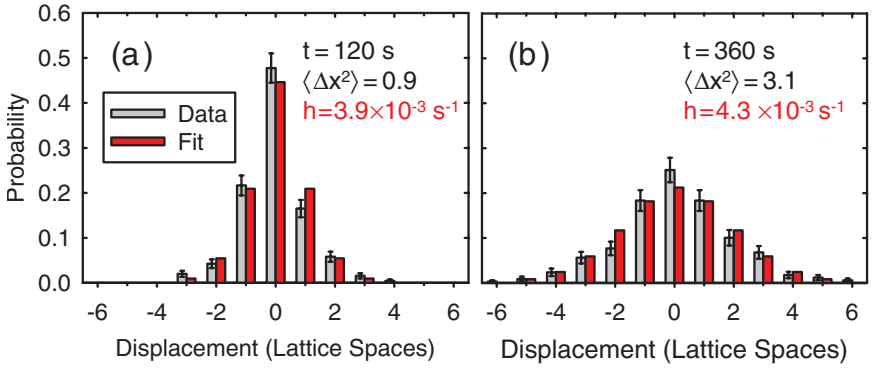

FIG. 2 (color). The displacement distribution (gray bars) for BBO_V's diffusion on $TiO_2(110)$ at 400 K obtained with two different sampling times t equal to 120 s (a) and 360 s (b). Different t's were employed to illustrate that the mean square displacement $\langle \Delta x^2 \rangle$ increases linearly with t as expected from a simple 1D random walk. The $\langle \Delta x^2 \rangle$ values are extracted using a simple statistical formula $\langle \Delta x^2 \rangle = \sum_i P_i x_i^2$ where P_i is the probability of finding the diffusing BBO_V at a number of lattice space displacements x_i. The $\langle \Delta x^2 \rangle$ and h values are further used to calculate the full probability distribution using Eq. (1) for each particular t as shown with red bars. The total number of analyzed events is ~500.

Since the observed vacancy diffusion is thermally activated, the hopping rate h is given by $h = \nu \exp(-E_b/k_B T)$, where E_b is the diffusion barrier, ν is the preexponential factor, and k_B is Boltzmann's constant. To extract the relevant kinetic parameters (E_b, ν) we perform an Arrhenius analysis and plot the logarithm of h as a function of reciprocal temperature in Fig. 3. This analysis yields a diffusion barrier, $E_b = 1.15 \pm 0.05$ eV, and a preexponential factor, $\nu = 1 \times 10^{12.2 \pm 0.6}$ s^{-1}.

To further understand the details of BBO_V diffusion we employ periodic DFT calculations to determine the diffusion barriers for different BBO_V configurations. A periodic slab three rutile unit cells deep along the [110] direction, one unit cell wide along the $[1\bar{1}0]$ direction, and two to seven unit cells long along the [001] direction was used to determine the BBO_V diffusion barrier along the BBO row. The calculated barrier height decreases marginally with increasing slab size as the BBO_V separation distance increases along the [001] from two to seven unit cells. Comparing the (6×1) and (7×1) cells the barrier decreases only slightly (1.05 to 1.03 eV) indicating convergence to the diffusion barrier for isolated, noninteracting BBO_V's. The calculated barrier is in very good agreement with our experimentally determined value of 1.15 eV. Additionally, the preexponential factor, determined on the basis of transition state theory [24], is 2.6×10^{13} s^{-1} in very good agreement with our experimentally determined value of $10^{12.2 \pm 0.6}$ s^{-1}. This indicates there is no significant entropy barrier along the diffusion coordinate. We have also calculated the BBO_V barrier for cross row diffusion and obtained a value of ~5 eV making this process too slow to be observed in our experiments.

Heuristically, we expect that the energetics of the BBO_V's will depend strongly on their spatial distribution since they retain excess negative charge [8]. The DFT calculations enable us to quantitatively determine these energetics for various BBO_V configurations. The potential energy surface calculated as a function of increasing BBO_V-BBO_V separation along the BBO row is shown in Fig. 4. The results show that the nearest neighbor and second nearest neighbor BBO_V-BBO_V distances are energetically highly unfavorable by ~1 eV and as such these configurations will not be populated at thermal equilibrium. Interestingly, simple visual inspection of the images in Fig. 1 reveals that along the BBO row, BBO_V pairs are never observed on adjacent sites. For a random distribution of noninteracting BBO_V's the probability of finding a paired BBO_V dimer is simply equal to the BBO_V coverage (mole fraction). For a surface having a vacancy concentra-

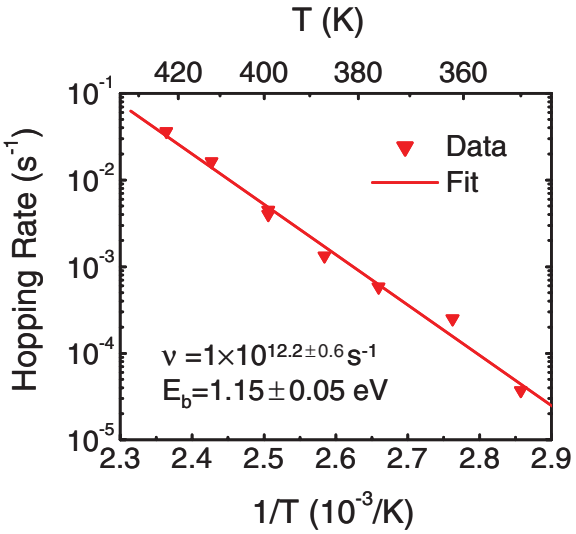

FIG. 3 (color). Arrhenius plot of hopping rates h calculated from the experimentally determined mean square displacements $\langle \Delta x^2 \rangle$ for diffusion of BBO_V's on $TiO_2(110)$. The statistical error bars are within the size of the symbols. The diffusion barrier and preexponential factor extracted from h are 1.15 ± 0.05 eV and $1 \times 10^{12.2 \pm 0.6}$ s^{-1}. The hopping rates reported here were determined by analysis of 300–1000 events.

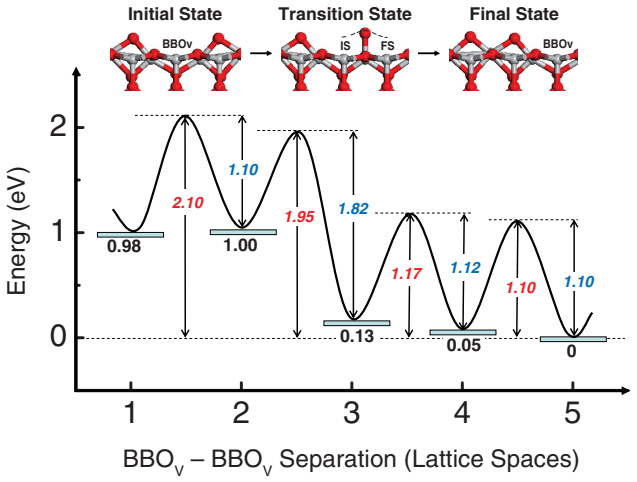

FIG. 4 (color). Calculated relative energy and diffusion barriers for BBO_V diffusion on $TiO_2(110)$ for a (9×1) model with two BBO_V's. The apparent diffusion of BBO_V's occurs by motion of the BBO ions along the [001] direction as shown in the schematic. In the transition state, the diffusing BBO is located directly on top of the underlying Ti^{4+} ion. Black (ground states) and red (transition states) numbers were calculated with respect to the ground state with the two BBO_V's separated by four BBO ions. Blue numbers are diffusion barriers required to decrease BBO_V-BBO_V separation by one BBO ion.

tion of 10% (such as the data presented in Fig. 1) we would expect 10% of the BBO_V's to exist as dimer pairs.

The BBO_V distribution along a given BBO row can be determined by analysis of the STM images. The distribution of BBO_V-BBO_V distances (not shown) shows a strong preference for BBO_V separations larger than 3 lattice spacings and demonstrates the presence of repulsive BBO_V-BBO_V interactions along the BBO_V rows in agreement with the DFT calculations presented here and those reported previously [6,7]. Despite the fact that BBO_V-BBO_V repulsion has been discussed theoretically [6,7], these repulsive interactions have not been quantified experimentally. The diffusion barrier for BBO_V-BBO_V distances of 4 and 5 lattice spacings are slightly higher ($\sim$7%) than the lowest value for the diffusion of isolated BBO_V of 1.03 eV.

In summary, we present the first study of the *intrinsic* mobility of bridge-bonded oxygen vacancies (BBO_V's) on a rutile $TiO_2(110)$ surface. Isothermal, atomically resolved STM images show that BBO_V's migrate along BBO atom rows. The hopping rate increases exponentially with increasing temperature with an experimental activation energy of 1.15 eV. Density functional theory calculations are in very good agreement giving an energy barrier for hopping of 1.03 eV. Both theory and experiment indicate a short-range repulsive interaction between vacancies on a given BBO row.

This work was supported by the U.S. Department of Energy Office of Basic Energy Sciences, Chemical and Material Sciences Division, Robert A. Welch Foundation (F-0032), and National Science Foundation (CHE-0412609). Q. G. acknowledges support from PNNL. The experimental work as well as the theoretical calculations were performed at W. R. Wiley Environmental Molecular Science Laboratory, a national scientific user facility sponsored by the Department of Energy's Office of Biological and Environmental Research located at Pacific Northwest National Laboratory (PNNL). PNNL is operated for the U.S. DOE by Battelle under Contract No. DEAC0676RLO 1830.

*Deceased.
†Corresponding author.
Zdenek.Dohnalek@pnl.gov

[1] V. E. Henrich and P. A. Cox, *The Surface Scienceof Metal Oxides* (Cambridge University Press, Cambridge, 1994).
[2] M. Valden, X. Lai, and D. W. Goodman, Science **281**, 1647 (1998).
[3] A. L. Linsebigler, G. Q. Lu, and J. T. Yates, Chem. Rev. **95**, 735 (1995).
[4] H. J. Freund, H. Kuhlenbeck, and V. Staemmler, Rep. Prog. Phys. **59**, 283 (1996).
[5] B. Li *et al.*, Science **311**, 1436 (2006).
[6] M. D. Rasmussen, L. M. Molina, and B. Hammer, J. Chem. Phys. **120**, 988 (2004).
[7] A. Vijay, G. Mills, and H. Metiu, J. Chem. Phys. **118**, 6536 (2003).
[8] C. Di Valentin, G. Pacchioni, and A. Selloni, Phys. Rev. Lett. **97**, 166803 (2006).
[9] U. Diebold, Surf. Sci. Rep. **48**, 53 (2003).
[10] S. Wendt *et al.*, Phys. Rev. Lett. **96**, 066107 (2006).
[11] O. Bikondoa *et al.*, Nat. Mater. **5**, 189 (2006).
[12] S. Wendt *et al.*, Surf. Sci. **598**, 226 (2005).
[13] R. Schaub *et al.*, Science **299**, 377 (2003).
[14] U. Diebold *et al.*, Surf. Sci. **411**, 137 (1998).
[15] G. Kresse and J. Furthmuller, VASP, the Guide, http://cms.mpi.univie.ac.at/vasp/vasp/vasp.html.
[16] G. Kresse and D. Joubert, Phys. Rev. B **59**, 1758 (1999).
[17] J. P. Perdew *et al.*, Phys. Rev. B **46**, 6671 (1992).
[18] J. Oviedo, M. A. San Miguel, and J. F. Sanz, J. Chem. Phys. **121**, 7427 (2004).
[19] G. Mills, H. Jonsson, and G. K. Schenter, Surf. Sci. **324**, 305 (1995).
[20] H. Jonsson, Annu. Rev. Phys. Chem. **51**, 623 (2000).
[21] See EPAPS Document No. E-PRLTAO-99-027737 for an atomically resolved movie of bridge-bonded oxygen vacancy diffusion on $TiO_2(110)$ surface at 400 K. For more information on EPAPS, see http://www.aip.org/pubservs/epaps.html.
[22] J. D. Wrigley, M. E. Twigg, and G. Ehrlich, J. Chem. Phys. **93**, 2885 (1990).
[23] A more complicated expression involving longer jumps has also been derived [22]. In our case such longer jumps are unimportant, since they would involve the concerted motion of multiple BBO ions in the same direction. DFT calculations indicate such concerted motions are energetically unfavorable (> 5 eV).
[24] G. H. Vineyard, J. Phys. Chem. Solids **3**, 121 (1957).